ACS APPLIED MATERIALS & INTERFACES

RESEARCH ARTICLE

www.acsami.org

Rheological Behavior of Clay−Nanoparticle Hybrid-Added Bentonite Suspensions: Specific Role of Hybrid Additives on the Gelation of Clay-Based Fluids

Youngsoo Jung,[†] You-Hwan Son,[†] Jung-Kun Lee,[*,†] Tran X. Phuoc,[‡] Yee Soong,[‡] and Minking K. Chyu[†]

[†]Department of Mechanical Engineering & Material Science, University of Pittsburgh, Pittsburgh, Pennsylvania 15261, United States

[‡]National Energy Technology Laboratory, U.S. Department of Energy, Pittsburgh, Pennsylvania 15236, United States

ABSTRACT: Two different types of clay nanoparticle hybrid, iron oxide nanoparticle clay hybrid (ICH) and $Al_2O_3-SiO_2$ nanoparticle clay hybrid (ASCH), were synthesized and their effects on the rheological properties of aqueous bentonite fluids in steady state and dynamic state were explored. When ICH particles were added, bentonite particles in the fluid cross-link to form relatively well-oriented porous structure. This is attributed to the development of positively charged edge surfaces in ICH that leads to strengthening of the gel structure of the bentonite susensions. The role of ASCH particles on the interparticle association of the bentonite fluids is different from that of ICH and sensitive to pH. As pH of ASCH-added bentonite suspensions increased, the viscosity, yield stress, storage modulus, and flow stress decreased. In contrast, at low pH, the clay suspensions containing ASCH additives were coagulated and their rheological properties become close to those of ICH added bentonite fluids. A correlation between the net surface charge of the hybrid additives and the rheological properties of the fluids indicates that the embedded nanoparticles within the interlayer space control the variable charge of the edge surfaces of the platelets and determine the particles association behavior of the clay fluids.

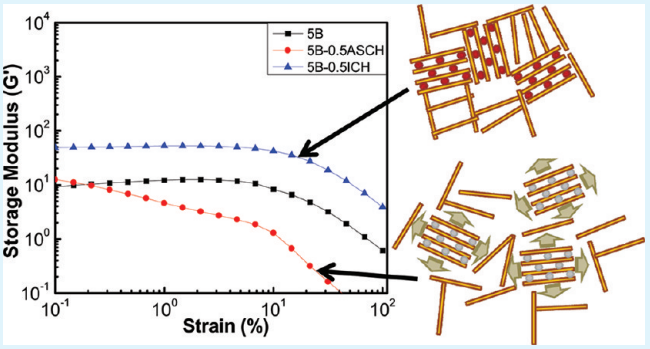

KEYWORDS: iron oxide intercalated clay hybrid, $Al_2O_3-SiO_2$ intercalated clay hybrid, rheological properties of bentonite suspension, clay particle interaction, pH effect, high temperature and high pressure

1. INTRODUCTION

Clay minerals are intensively utilized in a wide range of applications such as ceramic products, drilling fluids, molding sands, paints and paper industry.[1,2] Among the clay minerals, bentonite, a smectite type clay mineral, has attracted much attention because of its unique swelling ability, ion-exchange capacity, and rheological properties. In particular, the rheological properties of bentonite suspensions have been considerably studied. The most important factor to directly control viscosity, storage and loss modulus of clay suspensions is interparticle interaction. Plate-like clay particles are connected each other in the fluid through several modes: edge-to-face (E−F), edge-to-edge (E−E), and face-to-face (F−F) type coagulations of clay particles. A driving force of E−F type coagulation is an electrostatic force resulting from the negatively charged surface and the positively charged edges (E−F). Attraction between adjacent platelets by van der Waals forces leads to E−E or F−F type coagulation. To modify interparticle interaction, researchers have changed the ionic concentration[3−6] and pH[7−9] of the fluids. Additives such as organic surfactants,[10−12] polymers,[13−15] and nanoparticles[16,17] have been also added to the fluid as thickening agents.

Intercalation of nanoparticles into the interlayer space of clay can endow new functional properties to clay. Native clay minerals normally bind Na^+ and Ca^+ cations in the intragallery exchange sites. The replacement of the small cations by larger, more robust polycations and the subsequent thermal treatment transform the clay to the pillared clay. Inorganic pillared interlayered clays (PILCs) embedding Fe_2O_3, Al_2O_3, ZrO_2, TiO_2, ZnO, $SiO_2-Al_2O_3$, $Al_2O_3-Cr_2O_3$, SiO_2-TiO_2, and SiO_2-CoO nanoparticles have been successfully synthesized.[18−24] They are used in catalytic reaction, water purification, and sorption-based chemical separation.[25−27] However, the effect of these nanoparticles-intercalated clay particles as additives on the rheological properties of clay suspensions has not been investigated.

The objective of this work is to introduce effect of nanoparticles intercalated clay hybrid particles on montmorillonite suspensions and specific effect of pH on surface charging of montmorillonite suspensions containing clay hybrid particles. To the best of our knowledge, in a recent work, only the heterocoagulation process between montmorillonite and nanoparticles has been extensively studied, which reported the interaction of clay particles with oppositely charged inorganic oxide nanoparticles.[16,17]

In this paper, two different types of hybrid materials, iron oxide-clay hybrid (ICH) and $Al_2O_3-SiO_2$-clay hybrid (ASCH) were studied. We synthesized the hybrids and investigated

Received: June 8, 2011
Accepted: August 15, 2011
Published: September 02, 2011

dx.doi.org/10.1021/am200742b | *ACS Appl. Mater. Interfaces* 2011, 3, 3515–3522

their structural characteristics. In addition, we explored the effect of added hybrid particles on the rheological behavior of bentonite suspensions as a function of surface charge. Also, viscosity of prepared bentonite suspensions containing hybrid particles is examined in a high-temperature and -pressure environment.

2. EXPERIMENTAL PROCEDURE

2.1. Materials and Chemicals. Na^+−montmorillonite (Kunipia F, Kunimine Corp.) was used as starting material to fabricate metal oxide nanoparticle−clay hybrid particles. A chemical formula of Kunipia F is $Na_{0.35}K_{0.01}Ca_{0.02}(Si_{3.89}Al_{0.11})$ $(Al_{1.60}Mg_{0.32}Fe_{0.08})O_{10}(OH)_2 \cdot nH_2O$ and its cation exchange capacity (CEC) is 100 mequiv/100 g. Embedded nanoparticles were synthesized from $FeCl_3 \cdot 6H_2O$, $AlCl_4 \cdot 6H_2O$, $Si(OC_2H_5)_4$, and NaOH, which were obtained from SigmaAldrich and J.T. Baker. Aqueous clay fluids were prepared by mixing hybrid particles and bentonite ($H_2Al_2O_6Si$, CAS 1302−78−9, SigmaAldrich).

2.2. Synthesis of Nanoparticle−Clay Hybrids. In this study, two different types of nanoparticle−clay hybrid particles were prepared through the intercalation of metal polycations into the interlayer space of the clay and the subsequent thermal annealing. A detailed synthesis process of the hybrid particles is as follows.

2.2.1. Iron Oxide Clay Hybrid (ICH) Particles. Iron oxide clay hybrid (ICH) particles were synthesized following the procedure that was precisely described elsewhere.[18] Fe polycation solution was prepared by dissolving an aqueous solution of 0.2 M $FeCl_3 \cdot 6H_2O$ and that of 0.4 M NaOH at 70 °C. An intercalation process was carried out by mixing Fe polycation solution with Na^+- montmorillonite at 70 °C to intercalate Fe polycations into the interlayer space of Na^+- montmorillonite. The resulting particles were collected and excessive polycations on the surface were washed out with D.I. water several times. The hybrids were then dried and subsequently annealed at 450 °C in N_2 atmosphere to fully transform intercalated Fe polycations into embedded iron oxide nanoparticles.

2.2.2. Aluminosilicate Nanoparticle−Clay Hybrid (ASCH) Particles. We also prepared the hybrid particles in which aluminosilicate nanoparticles were embedded into the interlayer space of Na^+−montmorillonite. This is called Al_2O_3−SiO_2 clay hybrid (ASCH) particles. Al polycations solution was prepared by slowly mixing an aqueous solution of 0.2 M $AlCl_3 \cdot 6H_2O$ and that of 0.2 M NaCl. A molar ratio of OH^-/Al^{3+} in the Al polycation solution was 2.[28] The mixture solution was stirred vigorously for 24 h at room temperature and mixed with $Si(OC_2H_5)_4$ to prepare the aqueous hydroxy silico-aluminum polycation solutions in which the molar ratio of Al/Si is 1. This hydroxy silico-aluminum polycations were mixed with the Na^+−montmorillonite to intercalate prepared polycations into the interlayer space of Na^+−montmorillonite. After the intercalation process, the hybrid particles were washed, freeze-dried, and thermally annealed at 400 °C in N_2 atmosphere to fully convert the polycations into the aluminosilica nanoparticles.

2.3. Characterization of Hybrid Particles. Low-angle X-ray diffraction (XRD) measurement was performed to analyze the crystal structure of the nanoparticle-montmorillonite hybrids (Cu−Kα radiation, λ = 1.54 Å, Philips PW 1810 diffractometer). A change in *d*-spacing of the montmorillonite matrix was measured to monitor the intercalation of polycations and nanoparticles. Microstructure of the hybrid particles was also investigated by scanning electron microscope (SEM, JEOL-6610, Japan). In addition, to characterize the electrical layer on the surface of the particles, the zeta potentials of the bentonite and the hybrid particles in aqueous fluids were measured as a function of pH (ZetaPALS, Brookhaven, USA).

2.4. Preparation of Aqueous Fluids. To examine the effect of the hybrid particles on the rheological properties of clay-based fluids, we prepared the aqueous clay fluids by dispersing bentonite and hybrid particles in D.I. water. In aqueous fluids containing particle suspensions, bentonite (Aldrich, USA) was selected as a main clay component. After the solid particles were poured into D.I. water, the suspensions were agitated for 30 min by a mechanical stirrer and subsequently sonicated for 30 min by an ultrasonic horn. All processes were performed at room temperature. Solid contents in four different fluids were (i) 5 wt % bentonite (5B), (ii) 5 wt % bentonite and 0.5 wt % ASCH particles (5B-0.5ASCH), (iii) 5 wt % bentonite and 5 wt % ASCH particle (5B-5ASCH), and (iv) 5 wt % bentonite and 0.5 wt % ICH particles (5B-0.5ICH). To control the net surface charge of the particles in the fluids, we also adjusted the pH of the fluids by adding NH_4OH or HCl (J.T. Baker).

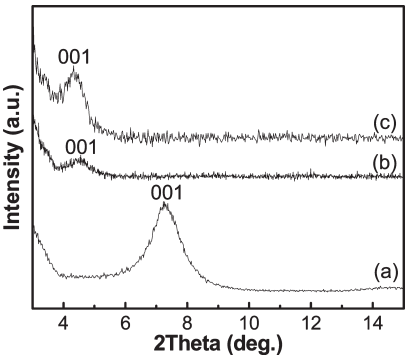

Figure 1. Low-angle X-ray diffraction patterns of pristine Na^+-montmorillonite and hybrid particles; (a) pristine clay, (b) as-grown ICH, and (c) as-grown ASCH particles.

2.5. Characterization of Rheological Properties. Influence of the hybrid particle additives on the rheological behavior was investigated by a rheometer (MCR 301, Anton paar, Austria) installed with a high-temperature, high-pressure (HTHP) cell. Measurements were performed at temperature ranging from 25 to 200 °C and at pressure between 1 and 100 bar. In the steady state measurement, the shear rate was increased from 1 to 200 s^{-1}. A step size was 4 s^{-1} and a duration time at each step was 10 s. In order to explore viscoelastic property of the fluids, a small amplitude oscillatory test was also carried out as the amplitude of the oscillatory strain increased from 0.001% to 100% at a fixed angular frequency, 10 rad/s. Prior to the oscillatory measurement, the fluids were presheared at the shear rate of 50 s^{-1} for 300 s and aged for 5 min.

3. RESULTS

3.1. Structure of ICH and ASCH Particles. Low angle XRD patterns of as-grown hybrid particles are shown in Figure 1. The interlayer spacing can be estimated from the basal spacing *d*(001) of the samples, which is determined from (00*l*) reflections in low-angle X-ray diffraction patterns. A change in the interlayer space of the intercalated hybrids estimated by tracking the position of (001) peaks provides strong evidence for intercalation of polycations.[29] Compared with pristine montmorillonite (Figure 1a), both ICH (Figure 1b) and ASCH (Figure 1c) particles show the shift of (001) peak to lower angle. The basal distance of 0.96 nm in pristine montmorillonite, was increased to 1.94 nm in ICH and 2.05 nm in ASCH. This expansion of the interlayer space indicates that Na^+ ions in the montmorillonite were successfully replaced with larger oxide nanoparticles in the hybrid particles. XRD results show that the size of embedded nanoparticles was about 2 nm after the intercalation process. Figure 2 shows high angle XRD patterns of the pristine montmorillonite and the hybrid particles. Additional reflections that

appeared in ICH, are indexed as the rhombohedral hematite phase (α-Fe_2O_3). This attests to the formation of the oxide nanoparticles within the interlayer space. In case of ASCH, no crystalline phase appeared after ASCH particles were annealed at 400 °C. In general, it has been reported that Al_2O_3 possessed high thermal stability, which initiated phase transformation from amorphous to γ-Al_2O_3 at 500−600 °C, and some oxide materials such as SiO_2, Cr_2O_3, and La_2O_3 inhibit phase transformation of Al_2O_3.[30−34] Therefore, the amorphous nature of aluminosilicate nanoparticles shows that Al and Si are uniformly mixed to form the solid solution.

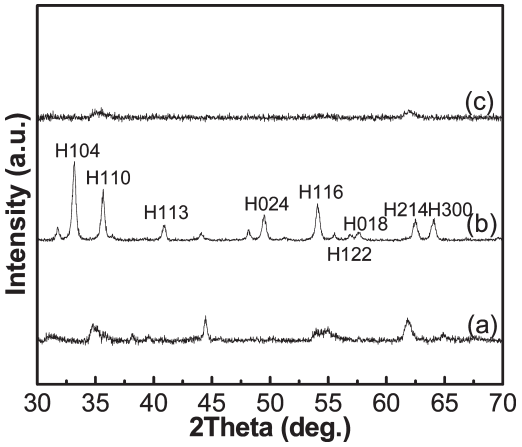

Figure 2. High-angle X-ray diffraction patterns of pristine Na^+-montmorillonite and hybrid particles: (a) pristine clay, (b) 450 °C annealed ICH, and (c) 400 °C annealed ASCH particles. (H: Hematite).

3.2. Microstructures of Clay Fluids Containing Hybrid Particles. The effect of the hybrid additives on the formation of the clay networks was examined by analyzing the microstructure of the solid suspension. To investigate the particle network in the suspension, the fluids were quickly frozen by pouring liquid nitrogen and the frozen solids were dried at −45 °C. This process enabled us to preserve the particle network in the suspension. Figure 3 shows scanning electron microscope (SEM) micrographs of the freeze-dried solids. The fluid consisting of only bentonite (Figure 3a) has an entangled ivy-like internal structure with the irregular shape of interparticle pores. When 0.5 wt % ASCH is added to 5 wt % bentonite suspension, the zigzag type connection of the clay particles disappeared and the clay particles were randomly stacked (Figure 3b). However, a very different internal structure of the solid is found in freeze-dried 5B-0.5ICH (Figure 3c). Individual platelike particles were cross-linked and a relatively well-oriented pore structure was developed.

3.3. Effect of Clay Hybrid Particles on the Rheologial Properties of Aqueous Clay Fluids. The flow behavior of any system is illustrated in terms of the relationship between the shear stress τ and the shear rate γ. The shear stress is stated precisely as the tangential force applied per unit area, and the shear rate is defined as the change of shear strain per unit time. The ratio of shear stress to shear rate is defined as viscosity η. In other words, η would be a measure of the resistance to flow of fluid suspension. Correlations between shear force and shear strain in fluids can be categorized as Newtonian, pseudoplastic, Bingham plastic, Bingham, and dilatant behaviors. The Newtonian which the shear stress is directly proportional to shear rate, reveals constant viscosity, whereas viscosity of other types of fluid behavior called non-Newtonian fluids could be varied with shear rate. In this study, the correlation between shear stress and

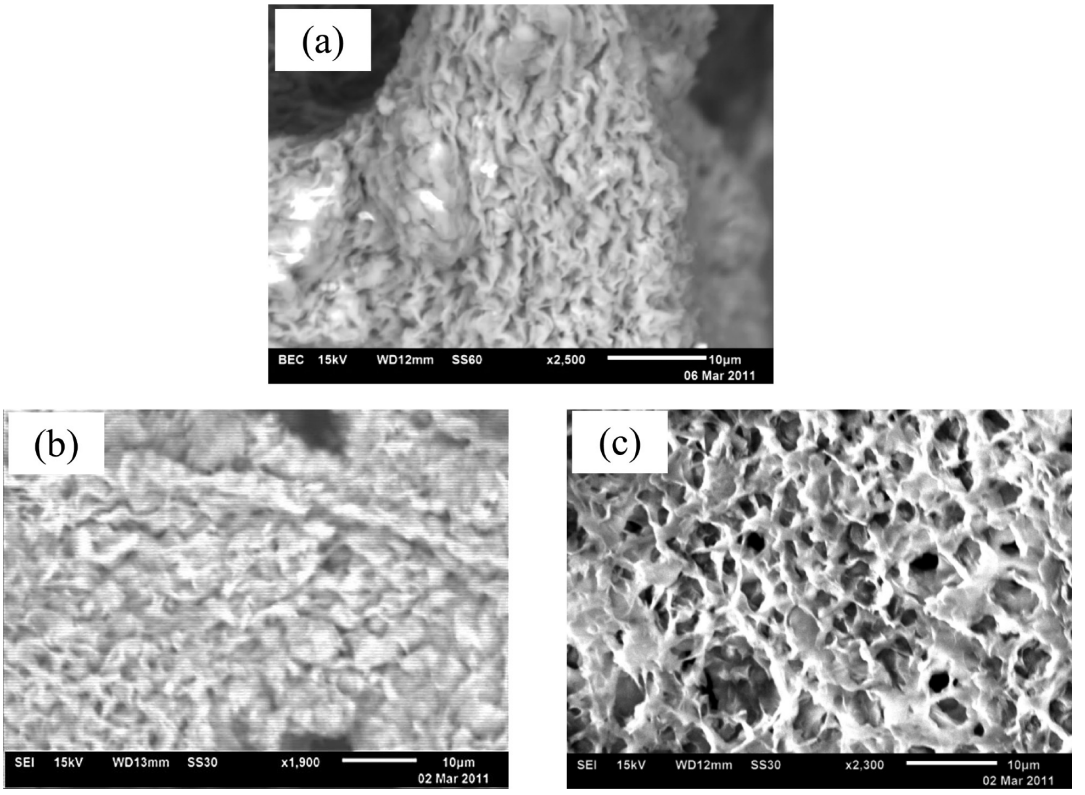

Figure 3. SEM micrographs of freeze-dried solids of (a) 5B, (b) 5B-0.5ASCH, and (c) 5B-0.5ICH.

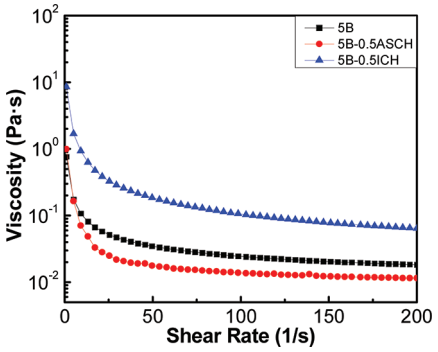

Figure 4. Viscosity vs shear rate curves of the fluid samples at 25 °C under atmospheric pressure.

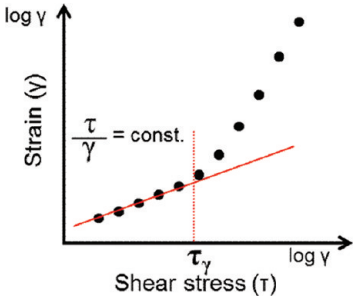

Figure 5. Schematic illustration of acquisition of yield point using the tangent in the linear-elastic deformation.

shear rate is explained by using the Bingham plastic behavior. The effect of the hybrid particles on the shear rate−viscosity correlation in the aqueous fluids under atmospheric pressure is presented in Figure 4. When NH_4OH or HCl was not added to the fluid additionally, pH of the fluids was in the range of 8−8.5. In comparison with the reference fluid (5B), the viscosity of 5B-0.5ICH suspension increased almost by one order of the magnitude. In contrast, the addition of 0.5 wt % ASCH into 5 wt % bentonite fluid decreased the viscosity of the fluid by about 50% as the shear rate increased from 20 to 200 1/s. The change in the yield stress also attests to the opposite effect of ICH and ASCH on the rheological properties. A yield point which is a transition point to a plastic flow shows the binding strength of the coagulated clay network structure in the fluid. The shear stress at the yield point was obtained by extrapolating shear stress vs shear strain curves as illustrated in Figure 5. The yield stress of 5B, 5B-0.5ICH, and 5B-0.5ASCH was 1.27, 0.98, and 12.05 Pa, respectively. The small amount of ICH additive significantly increased the yield stress, but the decrease in the yield stress was observed in 5B-0.5ASCH. High viscosity and yield stress of clay fluids are mainly due to the electrostatic attraction between negatively charged faces and positively charged edges of the platelike clay.[35] Hence, the dramatic change in the viscosity and yield stress of the fluids imply that the added hybrid particles modify the interparticle force in the clay suspension. As shown in Figure 3, the hybrid particles can develop a stable and robust gel network in the fluid. To scrutinize the interparticle interaction, the viscoelastic behavior of the fluid was measured by a small amplitude oscillatory test at a fixed angular frequency of 10 rad/s. Figure 6 shows the relation between storage modulus (G') and strain (ε). In the investigation of viscoelastic behavior of fluid systems, the

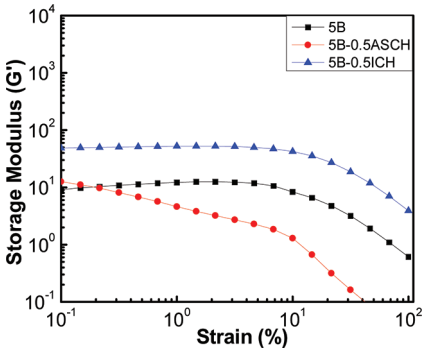

Figure 6. Storage modulus vs strain amplitude curves of the fluid samples at fixed frequency (10 rad/s).

storage modulus (G') and loss modulus (G'') represent elastic and viscous response of a given fluid system.[36] Storage modulus is related to the internal motion of material and the linear viscoelastic region that corresponds to a plateau in $G'-\varepsilon$ curve, represents the stability of fluid system.[37] G' of 5B-0.5ICH showing a long linear viscoelastic region (LVR) was 5−6 times larger than that of 5B in the range of strain from 0.1 to 100% . In contrast, $G'-\varepsilon$ curve of 5B-0.5ASCH did not show LVR and G' continuously decreased with an increase in ε. Longer LVR in 5B-0.5ICH suggests that the addition of ICH fortifies the coagulated network structure and enhances the stability of the clay suspension. ASCH oppositely influenced on the rheological properties of the clay suspension and turned the fluid to be more viscous. This trend is also observed in the flow stress of the clay suspension. Figure 7 presents the change in G' and G'' plotted in function of shear stress yielding from amplitude oscillatory test shown in Figure 6. In this plot, a critical point at which the storage modulus becomes equivalent to the loss modulus is called as a flow point. The shear stress at the flow point is the other way to determine the magnitude of external shear stress that is needed to transform the fluid from the elastic state to the viscous state.[37] Therefore, the strength of the interparticle interaction and the particle network in the fluids can be evaluated by monitoring the transition of the fluids from a solid-like elastic state to a liquid-like viscous state.[38] The flow stress increased from 1.44 Pa (5B fluid) to 8.02 Pa (5B-0.5ICH fluid). However, the flow stress for 5B-0.5ASCH was only 0.12 Pa, which is consistent with other measurement results suggesting that ACSH prevents the coagulation of the clay in the fluid and weakens the strength of the network structure.

3.4. Change in the Viscosity of the Clay Fluids at High Temperature and High Pressure. One of main applications of fluids containing clay particles is to control the rheology of water during the subterranean drilling. Therefore, there are interests on the change in the viscosity at high temperature and pressure, which is the condition of deep underground. Hence, we performed high-temperature and -pressure studies. In addition to the properties under atmospheric pressure at 25 °C, the viscosity of the clay suspensions was measured as a function of temperature at the pressure of 100 bar. Temperature dependence of the viscosity is shown in Figure 8. In pure bentonite fluid (Figure 8c), the increase in the temperature increased the viscosity and yield stress of the fluid, but the difference is not significant below 100 °C. This has been attributed to the fact that the change in the ionic activity at high temperature promotes the flocculation of the clay particles.[39,40]

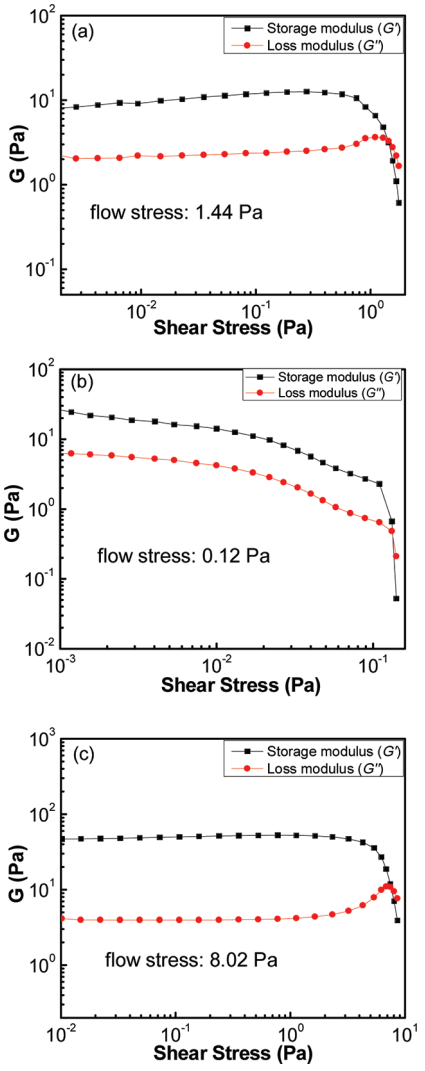

Figure 7. Change in storage (G') and loss modulus (G'') of fluid samples as a function of the shear stress; (a) 5B, (b) 5B-0.5ASCH, and (c) 5B-0.5ICH suspensions.

Briscoe et al. suggested that heating up the bentonite suspensions increased the conductivity of the fluid system, which is attributed to rise of Na^+ concentration dissolved from the surface of the particles. An increase in content of Na^+ by the raise of temperature leads to increase in yield stress and viscosity of clay suspensions.[4−6] As shown in panels a and b in Figure 8, the effect of high pressure is not as pronounced as that of high temperature, though the compression of the liquid media slightly increased the viscosity and yield stress of 5B and 5B-0.5ASCH.[39,41,42] The viscosity of 5B-0.5ICH was affected dominantly by increase in temperature. However, the addition of ASCH suppressed the increase in the viscosity and yield stress at high temperature. To confirm the role of ASCH additive, the amount of ASCH in the clay fluid was increased from 0.5 to 5 wt %. When 5 wt % of ASCH was added to 5 wt % bentonite fluid, the viscosity of the fluid increased slightly than that of 5B-0.5ASCH fluid and became independent of temperature. This suggests that addition of ASCH prevents the continuous gel structure of the clay and makes the clay particles well- dispersed even in the fluid of 200 °C with high ionic concentration.

3.5. Effect of pH on the Rheological Properties of Clay Fluids Containing Hybrid Particles. The change in the rheological properties of the clay fluids implies that the hybrid additives modify the coagulation behavior of the bentonite fluid. Given that the electrostatic interactions between platelike clay particles could be mainly affected by pH variation, we examined this hypothesis by varying pH of the fluids. The viscosity and yield stress of the fluids were measured as a function of pH, which is summarized in Figure 9 and Table 1. Compared with pure bentonite and ICH fluids, the viscosity and yield stress of ASCH fluid strongly depended on the pH of the fluid. Their viscosity and yield stress were larger at pH 5 than at pH 8 and 10 by more than one order of magnitude.

4. DISCUSSIONS

4.1. Evolution of Different Surface Charge on Hybrid Additives. The association of the platelike clay in water is attributed to the evolution of both positive and negative electric charges on the surface of the clay in fluids. The surface charge distribution of plate-like montmorillonite (or bentonite) consists of permanent negative charge at the face (charge-invariable) and pH-dependent positive charge at the edge (charge-variable). On the edge of platelets, the layers of octahedral Al−OH and tetrahedral Si−OH groups have broken links and dangling bonds at the end.[43] The broken links are amphoteric sites, because variable charges are conditionally developed at the edge. Concentrations of H^+ or OH^- which depend on the pH of the aqueous fluids, determine the polarity of the broken links. The evolution of the charge at the edge of the platelets under different pH is expressed as follows

$$\text{At low pH } ([H^+] > [OH^-]) : Al-OH + H^+ \rightarrow Al-OH_2^+ \quad \text{(positively charged edge surface)} \quad (1)$$

$$\text{At high pH } ([H^+] < [OH^-]) : Al-OH + OH^- \rightarrow Al-O^- \quad \text{(negatively charged edge surface)} \quad (2)$$

$$Si-OH + OH^- \rightarrow Si-O^- \quad \text{(negatively charged edge surface)} \quad (3)$$

A question of the interest is how the intercalation of the oxide nanoparticles changes the charge distribution of the hybrid particles. To inspect the variation of surface charge with respect to pH, we investigated the zeta potential of bentonite, ICH, and ASCH in 1 mM KCl electrolyte as a function of pH. Zeta potential can be utilized to estimate the effect of the particle charge on such as aggregation, flow, sedimentation, and filtration behaviors and also used to evaluate effect of various reagents on the properties of the colloid suspension.[44] Generally, colloidal particles with zeta potential >30 mV or zeta potential < −30 mV are considered stable. The results are shown in Figure 10. The zeta potential of the platelet clay particles is a net surface charge, which is determined by a difference between negative face charge and positive edge charge.[44] $Al_2O_3-SiO_2$ clay hybrid particles became more negatively charged in higher pH, which is in good agreement with eqs 1−3. In comparison, the negative charge of iron oxide clay hybrid particles exhibited marginal variation in a given pH range. The zeta potential of ASCH particles showed a dramatic decrease with an increase in pH and saturated at about −45 mV in pH ≥ 8. This variation can be explained by the surface charge of $Al_2O_3-SiO_2$ nanoparticles embedded within the interlayer of montmorillonite.[45] The surface charge of $Al_2O_3-SiO_2$

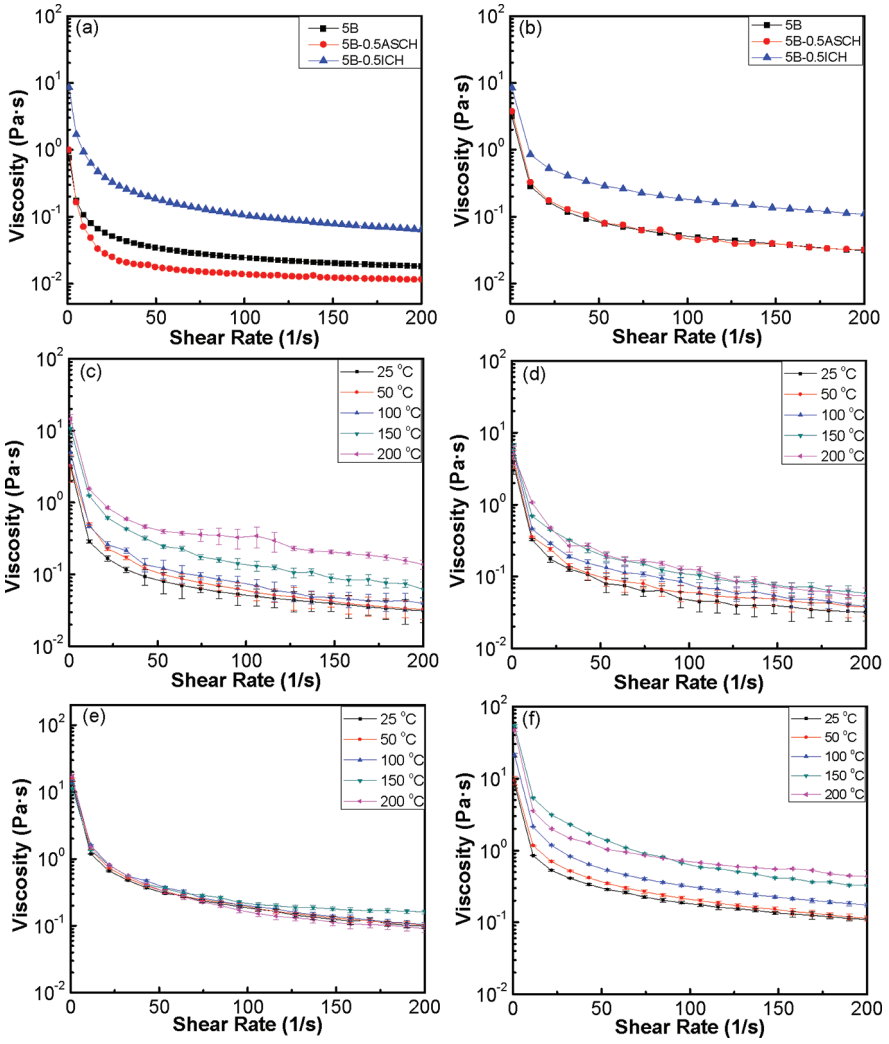

Figure 8. Viscosity vs shear rate curves of (a) samples 5B, 5B-0.5ASCH, 5B-0.5ICH at 25 °C and atmospheric pressure; (b) samples 5B, 5B-0.5ASCH, 5B-0.5ICH at 25 °C and 100 bar; (c) sample 5B, at 20−200 °C and 100 bar; (d) sample 5B-0.5ASCH, at 20−200 °C and 100 bar; (e) sample 5B-5ASCH, at 20−200 °C and 100 bar; and (f) sample 5B-0.5ICH at 20−200 °C and 100 bar.

nanoparticles stays negative at pH >2. This negatively charged surface of embedded $Al_2O_3-SiO_2$ nanoparticles makes the overall charge of ASCH particles to be more negative than that of pure montmorillonite particle. When Fe_2O_3 nanoparticles were intercalated, the surface charge of ICH particles became much more positive than that of ASCH particles in whole range of pH. This is attributed to the high isoelectric point (IEP) of Fe_2O_3 nanoparticles. Because the surface of Fe_2O_3 nanoaprticles is positively charged in water, the edge of ICH particles is positive even at pH ~8, where pure montmorillonite shows the negative charge at the edge surface. These results suggest that the surface charge of oxide nanoparticles intercalated within the interlayer of the clay particles has an important effect on the net charge of the hybrid particles through changing the charge at the edge surface.

4.2. Role of the Surface Charge of Hybrid Additives on the Gel Structure of the Clay Fluids. Differences in the net surface charge and pH dependence of the hybrid particles explain the role of the hybrid particles as rheology controlling additives in the aqueous bentonite fluids. The association of the clay platelets in the fluids occurs through several modes: edge-to-face (E-F), edge-to-edge (E-E), and face-to-face (F−F) flocculation.[46] F−F type association that brings about the precipitation of thick clay flakes weakens the gel strength because of (i) the decreased number of the clay particles that participate in constructing the gel structure and (ii) the decreased surface area of aggregate that is necessary for interplatelet interactions. In contrast, E−F and E−E association of platelets promote the gel-like structure and form the three-dimensional voluminous "house-of-card" structure within the fluid.[35] A correlation between the zeta potential and the viscosity in hybrid particle added bentonite fluids reveals that more negatively charged edge surface of the hybrids lowers the viscosity of the aqueous fluids. As shown in 5B-0.5ICH, the development of the positive charge at the edge surfaces that is manifested by the increase in the net surface charge, increases the viscosity and yield stress of the fluid. The positively charged edges of the hybrid additives produce attractive interactions with the negatively charged face of the bentonite, leading to the construction of the three-dimensional 'house-of-card' structures. However, more negatively charged edges of the hybrids generate a repulsive force between hybrid and bentonite particles and consequently prevent the coagulation and the network-structure formation in the bentonite fluid. As illustrated in

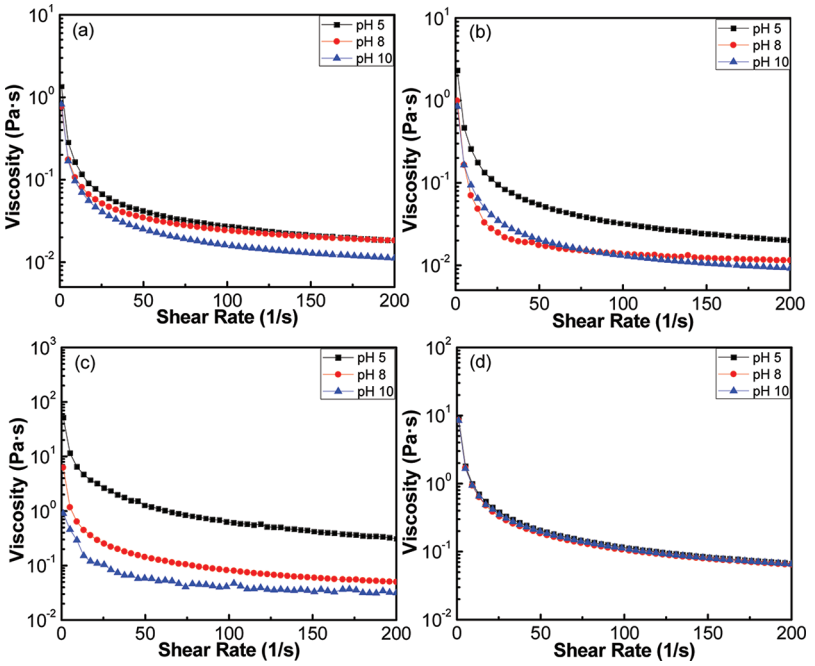

Figure 9. Viscosity vs shear rate curves of the fluid samples with respect to change of pH: (a) 5B, (b) 5B-0.5ASCH, (c) 5B-5ASCH, and (d) 5B-0.5ICH suspensions.

Table 1. Variation of Yield Stress of the Prepared Fluid Samples with Respect to Change of pH

	yield stress (Pa)		
fluids samples	pH5	pH8	pH10
5B	1.52	1.27	1.20
5B-0.5ASCH	2.91	0.98	0.91
5B-5ASCH	67.51	7.69	4.32
5B-0.5ICH	11.07	12.05	10.58

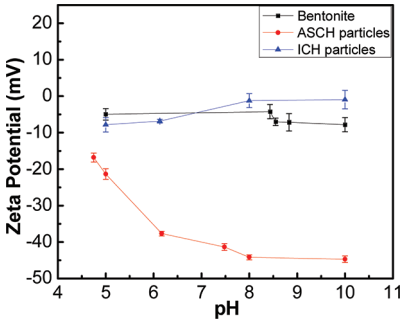

Figure 10. Variation of zeta potential of bentonite, ASCH, and ICH particles as a function of pH.

Figure 11, this repulsive interparticle force between negatively charged surfaces reduces both viscosity and yield stress, as shown in 5B-0.5ASCH at pH 8 and 10. For ICH particles, the variation of zeta potential at pH 5−10 was marginal and the stabilized positive charge at the edge surfaces strengthens E-F association. This explains the internal microstructure of 5B-0.5ICH showing the well-developed porous network that is the origin of its high viscosity and yield stress.

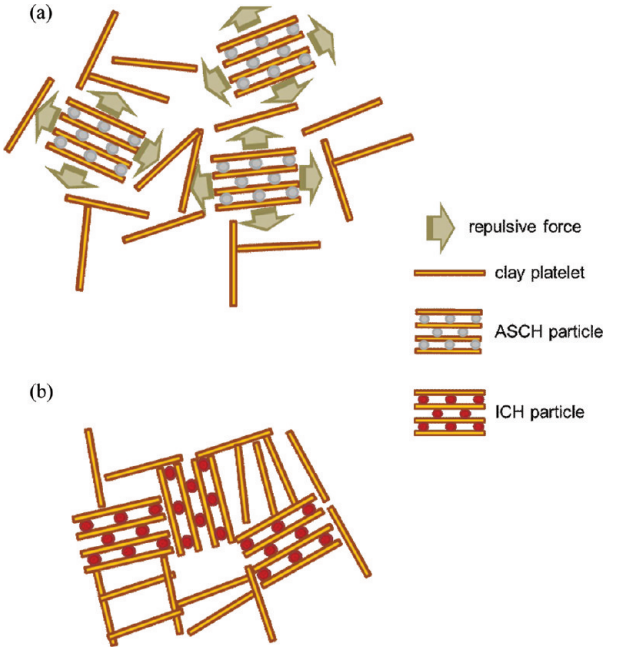

Figure 11. Schematic illustration of (a) particles association in 5B-0.5ASCH and (b) "house-of-card" structure in 5B-0.5ICH fluid.

5. CONCLUSIONS

We synthesize two different types of the nanoparticle − clay hybrid particles and investigate their effect on the rheological properties of aqueous bentonite fluids. In 5B-0.5ICH fluid, individual particles cross-link to develop a relatively well-oriented porous structure. The formation of the rigid gel structure makes a noticeable increase in the viscosity, yield stress, storage modulus,

and flow stress of the fluids. The strengthening of the gel structure by the addition of ICH particles results from the development of net positively charged edge surfaces in ICH. The role of ASCH particles on the clay platelets association in the bentonite fluids is sensitive to the change in pH. At high pH, the addition of ASCH into the bentonite suspension gives rise to the collapse of the pre-existing clay network and prevents the E−F type association of the platelets, leading to the decrease in the viscosity, yield stress, storage modulus, and flow stress. As pH of the fluid containing ASCH additives decreases, the clay in the suspension become flocculated and the rheological properties of the ASCH added fluid get close to those of the ICH added fluids. A correlation between the net surface charge of the hybrid additives and the rheological properties of the fluids indicates that the embedded nanoparticles within the interlayer space control the variable charge of the edge surfaces of the platelets and determine the association modes of the clay constituents in the fluids.

AUTHOR INFORMATION

Corresponding Author
*E-mail: jul37@pitt.edu.

ACKNOWLEDGMENT

This work was partially supported by the U.S. Department of Energy.

REFERENCES

(1) Grim, R. E. *Clay Minerology*, 2nd ed.; McGraw-Hill: New York, 1968; p 596.
(2) Fowden, L.; Barrer, R. M.; Tinker, P. B. *Clay Minerals; Their Structure, Behaviour and Use*; Royal Society Chemisty: London, 1984.
(3) Heller, H.; Keren, R. *Clays Clay Miner.* **2001**, *49*, 286.
(4) Ramos-Tehada, M. M.; Arrovo, F. J.; Peren, R.; Duran, J. D. G. *J. Colloid Interface Sci.* **2001**, *235*, 251.
(5) Tombácz, E.; Szekeres, M. *Appl. Clay Sci.* **2004**, *27*, 75.
(6) Laribi, S.; Fleureua, J. M.; Grossiord, J. L; Kbir-Ariguib, N. *Clays Clay Miner.* **2006**, *54*, 29.
(7) Missana, T.; Adell, A. *J. Colloid Interface Sci.* **2000**, *230*, 150.
(8) Abend, S.; Lagaly, G. *Appl. Clay Sci.* **2000**, *16*, 201.
(9) Lagaly, G.; Ziesmer, S. *Adv. Colloid Interface Sci.* **2003**, *100−102*, 105.
(10) Schott, H. *J. Colloid Interface Sci.* **1968**, *26*, 133.
(11) Kuznetsova, L. E.; Serb-Serbina, N. N. *Kolloidn, Zh.* **1968**, *30*, 853.
(12) Heath, D.; Tadros, Th. F. *J. Colloid Interface Sci.* **1983**, *93*, 307.
(13) Liu, P. *Appl. Clay Sci.* **2007**, *38*, 64.
(14) Manitiu, M.; Horsch, S.; Gulari, E.; Kannan, R. M. *Polymer* **2009**, *50*, 3786.
(15) Dykes, L. M. C.; Torkelson, J. M.; Burghardt, W. R.; Krishnamoorti, R. *Polymer* **2010**, *51*, 4916.
(16) Baird, J. C.; Walz, J. Y. *J. Colloid Interface Sci.* **2007**, *306*, 411.
(17) Tombácz, E.; Csanaky, C.; Illés, E. *Colloid Polym. Sci.* **2001**, *279*, 484.
(18) Son, Y. -H.; Lee, J. -K.; Soong, Y.; Martello, D.; Chyu, M. *Chem. Mater.* **2010**, *22*, 2226.
(19) Choy, J. -H.; Kwak, S. -Y.; Han, Y. -S.; Kim, B. -W. *Mater. Lett.* **1997**, *33*, 143.
(20) Walcarius, A.; Etienne, M.; Delacote, C. *Anal. Chim. Acta* **2004**, *508*, 87.
(21) Bois, L.; Bonhommé, A.; Ribes, A.; Pais, B.; Raffin, G.; Tessier, F. *Colloids Surf., A* **2003**, *221*, 221.
(22) Bourlinos, A. B.; Chowdhury, D. D.; An, Y. -U; Zhang, Q.; Archer, L. A.; Giannelis, E. P. *Small* **2005**, *1*, 80.
(23) Occelli, M. L. *J. Mol. Catal.* **1986**, *35*, 377.
(24) Occelli, M. L. In *Proceedings of the International Clay Conference*; Denver, Co, 1985; Clay Minerals Society: Chantilly, VA, 1985; p 319.
(25) Rightor, E. G.; Tzou, M. -S.; Pinnavaia, T. J. *J. Catal.* **1991**, *130*, 29.
(26) Xu, S. H.; Boyd, S. A. *Adv. Agron.* **1997**, *59*, 25.
(27) Breu, J.; Catlow, C. R. A. *Inorg. Chem.* **1995**, *34*, 4504.
(28) Gil, A.; Vicente, M. A.; Korili, S. A. *J. Catal.* **2005**, *229*, 119.
(29) Gil, A.; Gandia., L. M. *Chem. Eng. Sci.* **2003**, *58*, 3059.
(30) Jung, Y. -S.; Kim, D. -W.; Kim, Y. -S.; Park, E. -K; Baeck, S. -H. *J. Phys. Chem. Solids* **2008**, *69*, 1464.
(31) Bye, G. C.; Simpkin, G. T. *J. Am. Ceram. Soc.* **1974**, *8*, 367.
(32) Lin, Y. S. *J. Mater. Sci.* **1991**, *26*, 715–720.
(33) Gunay, V. In *Proceedings of the Third Euro-Ceramics Society Conference*; Madrid, Spain; European Ceramics Society: Bologna, Italy, 1993; p 267.
(34) Kumagi, M.; Messing, G. L. *J. Am. Ceram. Soc.* **1984**, C-230–C-231.
(35) Van Olphen, H. *Introduction to Clay Colloid Chemistry*, 2nd ed.; Wiley & Sons; New York, 1977.
(36) Zhang, L. -M.; Jahns, C.; Hsiao, B. S.; Chu, B. *J. Colloid Interface Sci.* **2003**, *266*, 339.
(37) Niraula, B.; King, T. C.; Misran, M. *Colloids Surf., A* **2004**, *251*, 59.
(38) Son, Y. -H.; Lee, J. -K.; Soong, Y.; Martello, D.; Chyu, M. *Appl. Phys. Lett.* **2010**, *96*, 121905.
(39) Briscoe, B. J.; Luckham, P. F.; Ren, S. R. *Trans. R. Soc. London, Ser. A* **1994**, *348*, 179.
(40) Luckham, P. F.; Rossi, S. *Adv. Colloid Interface Sci.* **1999**, *82*, 43.
(41) Van Olphen, H. *Proceedings of the Fourth National Conference on Clays and Clay Minerals*; University Park, PA, Oct 10−13, 1955; National Academy of Sciences: Washington, D.C., 1956; p 204.
(42) Alderman, N. J.; Gavignet, A.; Guillot, D.; Maitland, G. C. SPE 63rd Annual Technical Conference and Exhibition; Houston, TX, Oct 2−5, 1988; Society of Petroleum Engineers: Richardson, TX, 1988; p 187.
(43) Johnston, C. T.; Tombácz, E. *Soil Sci. Soc. Am. J.* **2002**, 37.
(44) Duman, O.; Tunc, Sibel. *Microporous Mesoporous Mater.* **2009**, *117*, 331.
(45) Gun'ko, V. M.; Zarko, V. I.; Leboda, R.; Chibowski, E. *Adv. Colloid Interface Sci.* **2001**, *91*, 1.
(46) Van Olphen, H. *J. Colloid Interface Sci.* **1964**, *19*, 313.